ELSEVIER

Physica D 144 (2000) 20–36

PHYSICA D

www.elsevier.com/locate/physd

Generic inflationary and noninflationary behavior in toy-cosmology

Cristián Huepe [a], Marc-Etienne Brachet [a,*], Fabrice Debbasch [b]

[a] *Laboratoire de Physique Statistique de l'École Normale Supérieure, associé au CNRS et aux Universités Paris 6 et 7, 24 rue Lhomond, 75231 Paris Cedex 05, France*

[b] *Laboratoire de Radioastronomie, ENS Ulm, 24 Rue Lhomond, 75231 Paris Cedex 05, France*

Received 26 March 1999; received in revised form 14 January 2000; accepted 27 January 2000
Communicated by U. Frisch

Abstract

Cosmological solutions of a toy homogeneous isotropic universe filled with a superfluid Bose condensate described by a complex scalar field (with relativistic barotropic fluid interpretation) are studied. The eigenvalues of the tangent map for the resulting Hamiltonian system are used to classify the phase space regions and to understand the typical toy-universe evolution. After a transient, inflation is obtained in the hyperbolic (real eigenvalues) region. This new independent eigenvalue-based inflationary criterion is shown to be compatible and complementary to the standard slow roll-over conditions. For the later evolution of the toy-universe, a family of adiabatic trajectories oscillating about a conventional cosmology filled with a relativistic fluid is obtained once the system falls into the elliptic (imaginary eigenvalue) regions. The corresponding thermodynamic functions are computed.

PACS: 98.80.Hw; 98.80.Cq; 05.30.Jp; 47.37.+q

Keywords: Cosmology; Inflation; Adiabatic invariance; Superfluid

1. Introduction

In a purely Galilean framework, the correct tool to describe a Bose condensate of scalar particles is naturally quantum field theory. It turns out that at vanishingly small temperature and for enough bosons present in the condensate, the system can be efficiently modeled by introducing a complex time-dependent wave-function (or first quantized field), which describes the common state of all bosons in the condensate and whose time-evolution is determined by the Gross–Pitaevskii [1,2] equation, also called the nonlinear Schrödinger equation. Since a Bose condensate is superfluid [3], it is natural to expect that one can recover from such a pure quantum formulation another hydrodynamical one, where the state of the condensate and its dynamics are described in a manner more congruent with the formalism usually adopted to study nondissipative barotropic fluids. This can be done by using the Madelung transformation [4,5] and is now well documented in the literature [6,7].

* Corresponding author. Tel.: +33-01-44-32-3761; fax: +33-01-44-32-3433.
E-mail address: brachet@lps.ens.fr (M.-E. Brachet).

0167-2789/00/$ – see front matter
PII: S0167-2789(00)00032-4

Some years ago, Debbasch and Brachet [8] started from the assumption that there were regions of space–time where a relativistic Bose condensate could be correctly modeled using a single classical complex scalar field and developed a relativistic analog of the Madelung transformation. More precisely, it was shown that, under a wide variety of circumstances, a charged Klein–Gordon field could be described in terms of usual relativistic hydrodynamical variables (spatial particle density, enthalpy density, 4-velocity, etc.) and that these variables obey dynamical equations which are essentially identical to those of an ideal barotropic relativistic fluid, except for supplementary quantum pressure terms, which are also present in the Galilean limit. Several solutions of these equations were also examined, using both field theoretical and hydrodynamical languages. Among them are, in Minkovski space–time, the exact vortex solution as well as linear and nonlinear acoustic waves, and in curved space–time, the static boson star, sometimes called soliton star.

A very special class of solutions to Einstein equations is constituted by the so-called cosmological solutions. Their frequent study is perhaps due to their physical importance and also to the fact that their simplest embodiment, the isotropic cosmologies, exhibit enough symmetry to be mathematically relatively tractable and still exhibit some nontrivial properties. It seems therefore quite natural to investigate, in both field theoretical and hydrodynamical languages, what kind of isotropic "universe" a charged Klein–Gordon field coupled to Einsteinian gravity could produce. This will mainly be done in the spirit of dynamical system theory. The links of this paper with physical cosmology will be discussed in Sections 4 and 5.

This paper is organized as follows. In Section 2, we derive the equations that are to be investigated. Section 3 introduces the main theoretical tool that will be used to qualitatively characterize the solutions of the cosmological equations and offers a generic picture of their possible behavior. Section 4 is devoted to a more thorough investigation of two important stages in the evolution of the toy-universe. In Section 5, we discuss our results and their links with the existing literature.

Finally, Appendix A rapidly reviews the correspondence between the field theoretical language used throughout the paper, and the hydrodynamical language, of interest for the physical interpretation of solutions discussed in Section 4.

Notation. Throughout this paper, the signature of the metric g is conventionally chosen to be negative and the physical dimension of $\mathrm{d}s^2 = g_{\mu\nu}\,\mathrm{d}x^\mu\,\mathrm{d}x^\nu$ will be $[\mathrm{d}s^2] = \mathrm{L}^2$.

2. Definition of the model

In this section, we present the main elements of the model, first for an arbitrary metric and field, and then for the particular case (relevant for a toy-cosmology) of the Friedman–Robertson–Walker (FRW) metric with a homogeneous field.

2.1. Fundamentals

In a general relativistic framework, we will consider the following Hilbert action for a complex scalar field Φ minimally coupled to the metric g [8,9]:

$$\mathcal{A} = \frac{1}{c}\int \sqrt{-\tilde{g}}\,\mathrm{d}^4x\left(\mathcal{L} - \frac{c^4}{16\pi G}R\right), \tag{1}$$

where the Lagrangian density is given by

$$\mathcal{L} = 2\alpha^2\nabla_\mu\Phi\nabla^\mu\Phi^* - 2\alpha f(|\Phi|^2), \tag{2}$$

with G the Newton gravitational constant, c the speed of light, $\tilde{g}$ the determinant of the metric tensor and R the scalar curvature of the Riemannian connection (Ricci's scalar) [9]. In the case of a Bose condensate of particles of rest mass m_b, the real positive constant α is given by $\alpha = \hbar/2m_\mathrm{b}$ with dimension $[\alpha] = \mathrm{L}^2\mathrm{T}^{-1}$. Requiring for the action that $[\mathcal{A}] = \mathrm{ML}^2\mathrm{T}^{-1}$ yields for the dimension of the matter field $[|\Phi|^2] = \mathrm{ML}^{-3}$. It is easy to show that, with these definitions, we have $[f(|\Phi|^2)] = \mathrm{ML}^{-3}\mathrm{T}^{-1}$.

In (2), the nonlinear character of the associated equations of motion for the scalar field Φ is contained in the polynomial function f. We define $f(r^2)$ by

$$f(r^2) = \frac{c^6}{8G\alpha^3}\sum_{i=1}^{n} f_i \left(\frac{4G\alpha^2}{c^4}r^2\right)^i, \tag{3}$$

where the constants G, c and α have been set so that the f_i are adimensional constants. In (3), the vacuum energy has been set to zero: $f(0) = 0$. This amounts to considering that no space–time curvature is induced by $\mathcal{L}$ when $\Phi = 0$. Note that the constant G cancels out only in the first term of f.

In order to push literal calculations as far as possible, we will sometimes particularize f to the following simpler form:

$$f(r^2) = \frac{c^2}{2\alpha} f_1 r^2 + \frac{2G\alpha}{c^2} f_2 r^4. \tag{4}$$

As we never consider in this paper nontrivial (i.e. symmetry breaking, Higgs-like) potentials, the essential content of our results will not depend on the f_2 term. Note that the formulas considerably simplify when $f_2 = 0$. However, we will retain a nonzero f_2 term in order to take into account generic nonlinear effects in the nonlinear Klein-Gordon (NLKG) equation.

The equation of motion for the matter field can be found by extremizing $\mathcal{A}$ with respect to Φ^*. This yields the NLKG equation (with polynomial nonlinearity):

$$\alpha\nabla_\mu\nabla^\mu\Phi + \Phi f'(|\Phi|^2) = 0. \tag{5}$$

The standard (linear) Klein–Gordon equation for particles without interaction is recovered from (5), keeping in mind that $\alpha = \hbar/2m_\mathrm{b}$, by setting $f_1 = \frac{1}{2}$ and all other f_i's to zero. However, f_1 will be kept as an arbitrary parameter throughout the text and fixed to $f_1 = \frac{1}{2}$ only to evaluate the results.

Extremizing $\mathcal{A}$ with respect to the metric furnishes the Einstein equations:

$$R^{\mu\nu} - \tfrac{1}{2}g^{\mu\nu}R = \frac{8\pi G}{c^2}T^{\mu\nu}, \tag{6}$$

where

$$T^{\mu\nu} = 2\alpha^2(\nabla^\mu\Phi^*\nabla^\nu\Phi + \nabla^\mu\Phi\nabla^\nu\Phi^*) - \mathcal{L}g^{\mu\nu} \tag{7}$$

is the energy–momentum tensor and $R^{\mu\nu}$ the contracted Ricci tensor [9]. This last expression, together with (5), completes the set of dynamical equations stemming from the stationary action principle for (1).

The complex field Φ is related to the real fields Θ and r by

$$\Phi = r\exp\left(\mathrm{i}\frac{\Theta}{2\alpha}\right). \tag{8}$$

As we describe in Appendix A, this expression can be used to produce a formal correspondence to a relativistic hydrodynamical flow through the Madelung transform [4,5]. In what follows, all expressions are given in terms of Θ and r.

2.2. Cosmological equations

In this section we consider the cosmological equations corresponding to our model of scalar field. Using the general relations found in the previous section, we will compute the characteristical scales and equations of motion for this particular toy-model.

Consider a homogeneous and isotropic FRW space–time model [9]:

$$\mathrm{d}s^2 = c^2\,\mathrm{d}t^2 - a^2(t)\left(\frac{\mathrm{d}l^2}{1-k\,l^2} + l^2\,\mathrm{d}\theta^2 + l^2\sin^2\theta\,\mathrm{d}\phi^2\right), \tag{9}$$

where $a(t)$ is the characteristic length scale of the universe and k is a discrete parameter that will control whether (9) produces a closed ($k=1$), a flat ($k=0$) or an open ($k=-1$) universe.

Let us now find the dynamical equations for a, r and Θ. Inserting the homogeneous field Φ and the FRW metric into (5), the real part of the product of the NLKG equation by Φ^* produces

$$r_{tt} + 3\frac{a_t\,r_t}{a} - r\frac{\Theta_t^2}{4\alpha^2} + \frac{c^2}{\alpha}r\,f'(r^2) = 0, \tag{10}$$

while, by using the imaginary part, we obtain

$$\partial_t(a^3 r^2\,\Theta_t) = 0, \tag{11}$$

from which we define the conserved quantity Π_Θ as

$$\Pi_\Theta \equiv \frac{1}{c^2}\,a^3 r^2\,\Theta_t. \tag{12}$$

Einstein equations become

$$\frac{a_t^2}{a^2} + \frac{kc^2}{a^2} = \frac{16\pi G\alpha^2}{3c^4}\left(r_t^2 + r^2\frac{\Theta_t^2}{4\alpha^2} + \frac{c^2}{\alpha}f(r^2)\right), \tag{13}$$

$$2\frac{a_{tt}}{a} + \frac{a_t^2}{a^2} + \frac{kc^2}{a^2} = -\frac{16\pi G\alpha^2}{c^4}\left(r_t^2 + r^2\frac{\Theta_t^2}{4\alpha^2} - \frac{c^2}{\alpha}f(r^2)\right). \tag{14}$$

Eqs. (10), (11), (13) and (14) form a seemingly overdetermined system for only three independent variables (a, r and Θ). To better understand the status and compatibility of these equations, let us consider the dynamical system defined by the Lagrangian

$$L = \frac{3ca}{8\pi G}(-a_t^2 + kc^2) + \frac{2\alpha^2 a^3}{c^3}\left(r_t^2 + r^2\frac{\Theta_t^2}{4\alpha^2} - \frac{c^2}{\alpha}\,f(r^2)\right), \tag{15}$$

which stems from the action $\mathcal{A}$ when the matter field variables and the FRW metric are directly replaced into (1). Eq. (11) then results from the Noether conserved current associated with the $U(1)$ invariance of L while (13) is obtained by setting to zero the conserved "energy" $E = \partial L/\partial q_t - L$. Eqs. (10) and (14) are obtained by combining the Euler–Lagrange equations for L with (13). The conservation equations (11) and (13) must therefore be compatible with (10) and (14), which stem from the equations of motion. Note that the $E=0$ condition has to be imposed as a constraint, compatible with the dynamics stemming from (15). The reason being that the g^{tt} variation in (1) has no equivalent in (15).

Before we continue any further, let us introduce the natural units of the toy-model. Using α and c, the length and time units can be respectively defined by $L = 2\alpha/c$ and $T = 2\alpha/c^2$. For a Bose–Einstein condensate with bosons

of mass m_b, we have $\alpha = \hbar/2m_b$, and so L and T are respectively given by the Compton length ($l_c = \hbar/m_b c$) and time ($t_c = \hbar/m_b c^2$). A second natural scale is fixed by the gravitational constant G in the Riemannian curvature term of $\mathcal{A}$. We have chosen to define the mass unit as $M = 2\alpha c/G$ in order to deal with the Compton scale and G in the same system of units. For a Bose condensate, $M = M_p^2/m_b$ (where $M_p = \sqrt{\hbar c/G}$ is Planck's mass). We therefore define the following adimensional quantities that will be systematically used in Sections 3 and 4: $\tilde{t} = t/T$, $\tilde{a} = a/L$, $\tilde{r} = rL^3/M$, $\tilde{\Theta} = \Theta T/L^2$ and $\tilde{\Pi}_\Theta = \Pi_\Theta/M$. In these units, the adimensional constants $\{f_i\}$ are the only parameters of the model.

3. Phase space partition using eigenvalues of the tangent map

This section is devoted to the study of the dynamical system defined by the Lagrangian in (15) that describes the evolution of the toy-cosmology presented in Section 2. A partition of the phase space using the eigenvalues of the tangent map is presented. The resulting *eigenvalue-criteria* regions are then used to describe the evolution of a characteristic trajectory. From now on, we will use the adimensionalized variables $\tilde{t}$, $\tilde{a}$, $\tilde{r}$, $\tilde{\Theta}$ and $\tilde{\Pi}_\Theta$. However, the tildes will be omitted to simplify the notation.

3.1. Eigenvalues of the tangent map

While studying the vorticity (passive scalar) field equations in an inviscid, incompressible two-dimensional fluid, Weiss stressed the importance (for the qualitative understanding of trajectories) of the linearized evolution equation for the separation between nearby points in the phase space [10]. The eigenvalues of the tangent map allowed him to distinguish between hyperbolic and elliptical regions (corresponding to a pair of respectively real or purely imaginary eigenvalues). He observed that in the real eigenvalue regions the vorticity field is stretched in one direction while compressed in the perpendicular one, and that in the imaginary eigenvalue regions the vorticity tends to rotate without major deformations. The purpose of the rather long computation that is carried out in this section is to generalize this procedure to the dynamical system defined by the Lagrangian (15) in order to partition the associated phase space into four eigenvalue-criteria regions.

From (15) and the conserved quantity Π_Θ in (12), we obtain the following adimensionalized Hamiltonian:

$$H = -\frac{3k}{8\pi}a - \frac{2\pi\Pi_a^2}{3a} + \frac{\Pi_r^2}{2a^3} + \frac{\Pi_\Theta^2}{2a^3r^2} + a^3 f(r^2). \tag{16}$$

Here, the canonical conjugate momenta are defined by: $\Pi_r = \partial L/\partial r_t = a^3 r_t$ and $\Pi_a = \partial L/\partial a_t = -3aa_t/4\pi$. The Hamiltonian H thus provides a four-dimensional dynamical system for a, r, Π_a and Π_r. This system is further constrained to evolve only on the hypersurface defined by $H = 0$ as explained in the preceding section. We will use this constraint to represent the phase space in a three-dimensional volume by eliminating one of the degrees of freedom. We therefore define a *reduced* phase-space having as coordinates a, r and r_t.

Using simplectic coordinates and defining $\eta = (a, r, \Pi_a, \Pi_r)$, Hamilton's equations become $\dot{\eta}_i = J_{ik}\partial H/\partial\eta_k$ (the dot indicates a time derivative), where

$$J = \begin{bmatrix} 0 & I \\ -I & 0 \end{bmatrix} \tag{17}$$

with I the 2×2 identity block matrix. The elements of the tangent map matrix M of the vector field $\dot{\eta}_i$ are then given by

$$M_{ij} \equiv \frac{\partial\dot{\eta}_i}{\partial\eta_j} = J_{ik}\frac{\partial^2 H}{\partial\eta_j\partial\eta_k}. \tag{18}$$

The separation vector between two (asymptotically close) points in the phase space $\delta\eta_i$ follows the dynamical equation $\delta\dot{\eta}_i = M_{ij}\delta\eta_j$. Therefore, in the special case where M is constant, real eigenvalues correspond for $\delta\eta_i$ to an exponential behavior in time, while imaginary eigenvalues of M correspond to an oscillatory dynamics. In the general case, for a nonconstant M, the trajectories will behave exponentially in regions where the eigenvalues are real, and will be of an oscillatory nature in regions where the eigenvalues are imaginary.

The four eigenvalues for the tangent map matrix of the Hamiltonian (16) are obtained (after a straightforward calculation) as the solutions of the following characteristic bisquare polynomial expression:

$$\lambda^4 + B\lambda^2 + C = 0, \tag{19}$$

where B and C are given by

$$B = \frac{1}{a^6}\left(-8\pi\Pi_r^2 + \Pi_\Theta^2\left(\frac{3}{r^4} - \frac{8\pi}{r^2}\right)\right) + \left(-8\pi f + 2f' + 4r^2 f''\right), \tag{20}$$

$$\begin{aligned}\frac{C}{4\pi} = {} & \frac{3\Pi_\Theta^2}{a^{12}}\left(\frac{-\Pi_\Theta^2}{r^6} + \frac{\Pi_r^2}{r^4}\right) + \frac{\Pi_\Theta^2}{a^6}\left(\frac{-6f}{r^4} + \frac{8f'}{r^2} - 8f''\right) \\ & + \frac{\Pi_r^2}{a^6}(2f' + 4r^2 f'') - 4(ff' - 3r^2 f'^2 + 2r^2 ff'').\end{aligned} \tag{21}$$

We now proceed to explain in detail the bifurcations of the four solutions (λ_+, λ_-, $\tilde{\lambda}_+$, $\tilde{\lambda}_-$) of Eq. (19), since they will turn out to be of paramount importance to classify the phase space regions. Note that these are the standard bifurcations of a 4×4 symplectic matrix [11]. The explicit solutions of (19) are

$$\lambda_\pm = \frac{\pm(-B + \sqrt{B^2 - 4C})^{1/2}}{\sqrt{2}}, \qquad \tilde{\lambda}_\pm = \frac{\pm(-B - \sqrt{B^2 - 4C})^{1/2}}{\sqrt{2}}. \tag{22}$$

When $B^2 - 4C \geq 0$, both parentheses take real (positive or negative) values. All eigenvalues are then purely real or purely imaginary and symmetric with respect to the axes on the complex plane. These configurations are pictured in Fig. 1 and labeled by i, ii or iv. It is clear that at least one pair of eigenvalues must vanish at the frontiers between i, ii and iv, which will therefore be found at the surfaces where $C = 0$. On the other hand, when $B^2 - 4C < 0$,

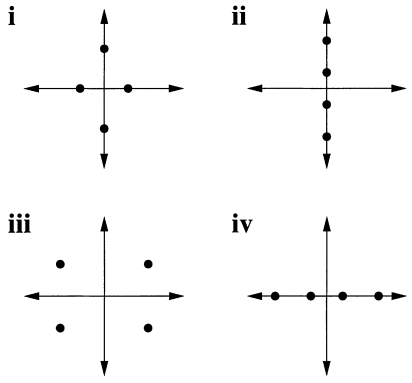

Fig. 1. All possible distributions on the complex plane of the four eigenvalues of the tangent map (see Eqs. (18), (19) and (22)): two real and two imaginary (i), four purely imaginary (ii — elliptic), four complex (iii) or four real (iv — hyperbolic) eigenvalues. Note that all possible configurations are symmetric with respect to the axes (see Section 2).

the parentheses take complex values so the eigenvalues cannot be situated on (but are still symmetrical with respect to) the axes in the complex plane. In this case (labeled by iii in Fig. 1), the frontier is directly given by the surface $B^2 - 4C = 0$. Let us point out that the symmetry with respect to the complex plane axes exhibited by all four eigenvalue configurations is due to the Hamiltonian nature of the problem. Indeed, since H, η and M are real, eigenvalues must appear in complex conjugate pairs. Furthermore, the time reversal symmetry of the Hamiltonian indicates that if λ is an eigenvalue, $-\lambda$ is also an eigenvalue.

In order to provide explicit expressions for (20) and (21), we use the minimal nonlinear form for f given in (4): $f(r^2) = f_1 r^2 + f_2 r^4$. We represent B and C in the reduced phase-space coordinates a, r and r_t:

$$B = -8\pi r_t^2 + \frac{\Pi_\Theta^2}{a^6}\left(\frac{3}{r^4} - \frac{8\pi}{r^2}\right) - 8\pi f_2 r^4 + (12 f_2 - 8\pi f_1) r^2 + 2 f_1, \tag{23}$$

$$\frac{C}{4\pi} = \left(\frac{3\,\Pi_\Theta^2}{a^6\, r^4} + 12\, f_2\, r^2 + 2 f_1\right) r_t^2 - \frac{3\,\Pi_\Theta^4}{a^{12} r^6} + \frac{\Pi_\Theta^2}{a^6}\left(\frac{2 f_1}{r^2} - 6 f_2\right) + 2r^2(6\, f_2\, r^4 + 10 f_1 f_2\, r^2 + 4 f_1^2). \tag{24}$$

We can then solve $C = 0$ and $B^2 - 4C = 0$ for r_t to find explicitly the frontiers between the various eigenvalue-criteria zones. We will not reproduce here the resulting literal expressions since they are extremely long and can be trivially recovered from (23) and (24).

3.2. Partition of the phase space

In Fig. 2, we show the frontiers on the reduced phase-space for $f_1 = f_2 = \frac{1}{2}$ and $\Pi_\Theta = 10$ first in the 3D space (Fig. 2A) and then on three cuts at fixed $a = 1$, $a = 5$ and $a = 1000$ (Fig. 2B–D, respectively). Each resulting region contains one of the different eigenvalue distributions (i, ii, iii or iv) pictured in Fig. 1 and has been labeled consequently. In Fig. 2A, the light surface correspond to the solutions of $C = 0$, and the two dark surfaces to $B^2 - 4C = 0$. In Fig. 2B–D, the dashed lines denote $C = 0$ and the solid ones, $B^2 - 4C = 0$.

In Fig. 2A, we define $a \sim a_{\mathrm{TI}}$ as the minimum a for which the elliptic zone ii contains a region with $r_t = 0$. It is apparent that there exists a *transition interval* for $a \sim a_{\mathrm{TI}}$, where all zones form an entangled 3D structure. For $a < a_{\mathrm{TI}}$, the reduced phase-space is essentially partitioned by the $C = 0$ surface, and for $a > a_{\mathrm{TI}}$, by the $B^2 - 4C = 0$ surface. From (23) and (24) it is straightforward to show that a_{TI} is given by $\Pi_\Theta / a_{\mathrm{TI}}^3 = \rho_{\mathrm{c}}(f_1, f_2)$, where $\rho_{\mathrm{c}}(f_1, f_2)$ is a long polynomial expression in f_1 and f_2. By evaluating $\rho_{\mathrm{c}}(f_1, f_2)$ we obtain $a_{\mathrm{TI}} \approx 2.6$ for the $\Pi_\Theta = 10$ case shown in the figure.

As a goes to 0, the r_t coordinate of all surfaces diverge, following the self similar law $r_t(a, r) \sim (\Pi_\Theta / a^3)\tilde{r}_t(r)$, where $\tilde{r}_t(r)$ are functions depending only on r that define the frontier surfaces on the (a, r) plane. Their shape is shown in Fig. 2B. In particular, the $C = 0$ surface follows the simple relation $r_t = \pm \Pi_\Theta / a^3 r$. At the transition interval ($a \sim a_{\mathrm{TI}}$), zone iii reaches the r axis and the $C = 0$ frontier becomes the nearest to the $r = 0$ axis (see Fig. 2C). Finally, for $a > a_{\mathrm{TI}}$, the condition $C = 0$ is only verified in a small region for which the r coordinate goes to 0 as $r \sim \Pi_\Theta / a^3$ (see Fig. 2D). Only the $B^2 - 4C = 0$ surface is therefore relevant. For $a \gg a_{\mathrm{TI}}$, we can neglect the Π_Θ / a^3 terms to obtain the following expression for this surface:

$$r_t^2 = f_2 r^4 + \left(-f_1 + \frac{3 f_2}{\pi}\right) r^2 + \frac{f_1}{2\pi} \pm \sqrt{\frac{6}{2^8 \pi^3}}\left[\frac{f_1^2}{8\pi} + \left(f_1 + \frac{3 f_2}{2\pi}\right) f_1 r^2 + \left(f_1 + \frac{9 f_2}{2\pi}\right) f_2 r^4 + 2(1 - f_2) f_2 r^6\right]^{1/2}. \tag{25}$$

The zeros of (25), as can be seen by inspection of Fig. 2D, define two relevant density scales (r_{C1} and r_{C2}) for r. For the parameters of Fig. 2 we numerically compute $r_{\mathrm{C1}} \approx 0.093$ and $r_{\mathrm{C2}} \approx 1.37$.

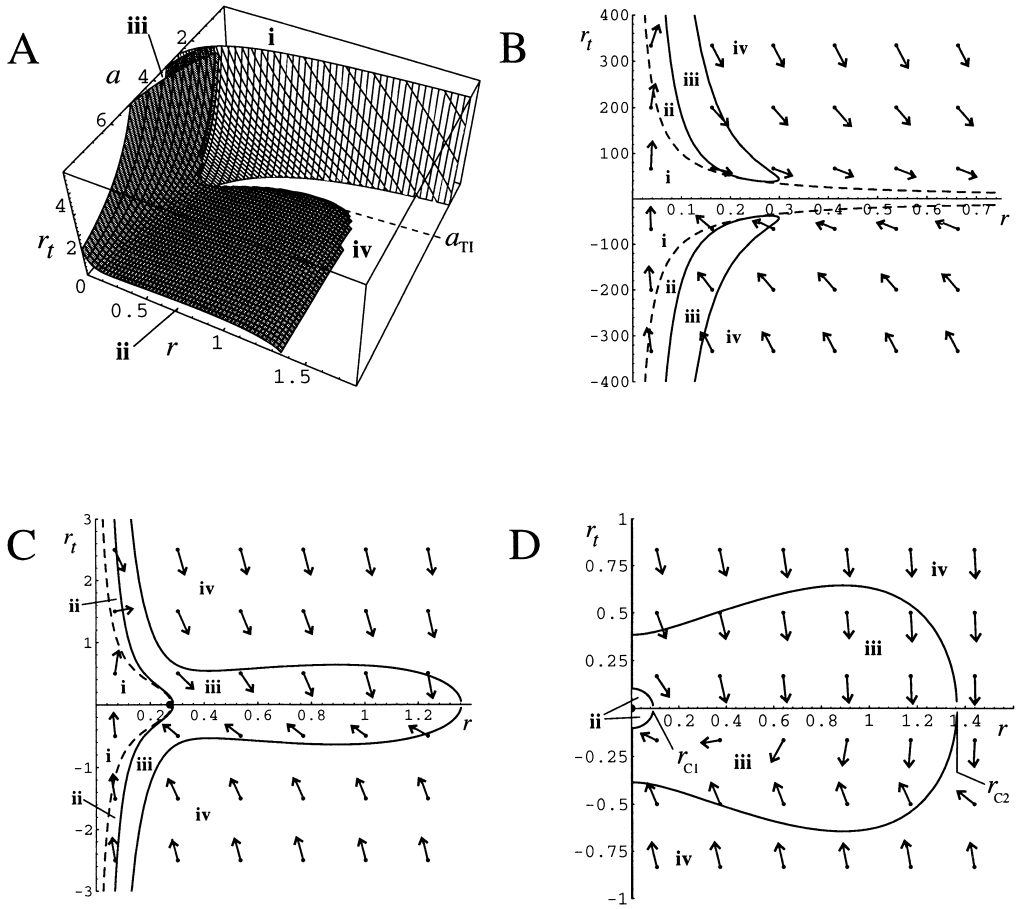

Fig. 2. Eigenvalue distribution in the reduced phase-space (labeled i–iv as in Fig. 1) with $\Pi_\Theta = 10$, $f(r^2) = f_1 r^2 + f_2 r^4$ and $f_1 = f_2 = \frac{1}{2}$. (A) Frontiers of zone iii (gray surface) and between zones i and ii or zones i and iv (white surface). The $r_t < 0$ region (not shown) is symmetric with respect to $r_t = 0$ to the presented half-space. (B)–(D) Two-dimensional cuts of the reduced phase-space A with $a = 1$ (B), $a = 5$ (C) and $a = 1000$ (D). The solid lines represent the gray frontiers and the dashed lines the white surface. The (normalized) vector field is the projection of the flow direction of trajectories on the B, C and D planes.

The analysis of the eigenvalue-criteria regions therefore provides us with three characteristic scales as functions of f_1 and f_2: $\Pi_\Theta/a_{\mathrm{TI}}^3$, r_{C1} and r_{C2}.

It is interesting to point out that the speed of sound c_{s} and the coherence length ξ, that we introduced in Eqs. (A.14) and (A.15) as the two natural constants appearing in the hydrodynamical interpretation, do not fix any of these characteristic scales. Furthermore, since they both depend on r, they cannot fix any scale on the reduced phase-space. Therefore, they do not parametrize the eigenvalue regions as one could have expected.

3.3. Forbidden zone

Another important feature of the reduced phase-space is the well-known forbidden zone [12,13] that appears when $k = +1$. It is defined as the region where the $H = 0$ condition cannot be satisfied. It can be found directly

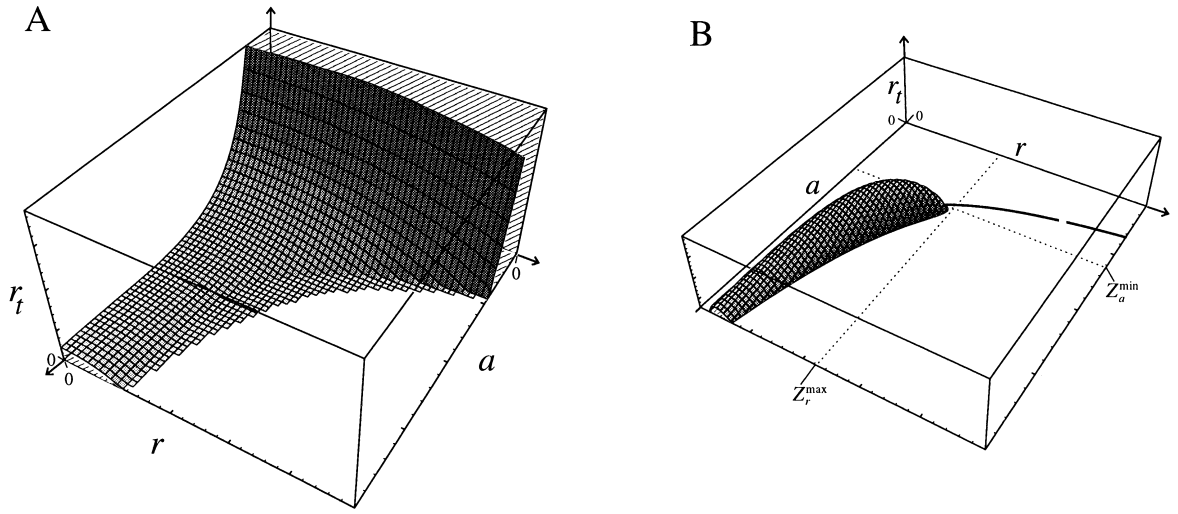

Fig. 3. Qualitative disposition of the forbidden region on the reduced phase-space with $f(r^2) = f_1 r^2 + f_2 r^4$, $f_1 = f_2 = \frac{1}{2}$ and $\Pi_\Theta = 0$ (A) or $\Pi_\Theta \neq 0$ (B). In (B), $Z^r_{\max}$ and $Z^a_{\min}$ indicate the r and a limits of the forbidden region. The dashed line plotted on the $r = 0$ surface shows the position of the minimum r_0 of the potential $V_{\text{eff}}(r^2)$ in Eq. (26).

from (16) by considering the zone where the effective potential

$$V_{\text{eff}}(r^2) = -\frac{3k}{8\pi}a - \frac{2\pi\Pi_a^2}{3a} + \frac{\Pi_\Theta^2}{2a^3 r^2} + a^3 f(r^2) \tag{26}$$

is lower or equal to zero, a condition equivalent to

$$r_t^2 + \frac{\Pi_\Theta^2}{a^6 r^2} + 2 f(r^2) < \frac{3}{4\pi a^2}. \tag{27}$$

In Fig. 3, we picture the forbidden zone on the reduced phase-space for $f(r^2) = f_1 r^2 + f_2 r^4$ with $f_1 = f_2 = \frac{1}{2}$. If $\Pi_\Theta = 0$ (Fig. 3A), the forbidden zone exists for all values of a, shrinking as the size a of the toy-universe grows with expansion. If $\Pi_\Theta \neq 0$ (Fig. 3B) the forbidden zone is bounded by $Z_a^{\min}$ and $Z_r^{\max}$ (see figure).

In Fig. 3B, we have also plotted a dashed line indicating the position in the (a, r) plane of the minimum of $V_{\text{eff}}(r^2)$. Note that this line must meet the surface of the forbidden zone at $a = Z_a^{\min}$ since the minimum of $V_{\text{eff}}(r^2)$ must be the first point to reach $V_{\text{eff}}(r^2) \leq 0$ as we vary a. Let us now find $Z_a^{\min}$ and $Z_r^{\max}$ as functions of Π_Θ. For $f(r^2) = f_1 r^2 + f_2 r^4$, using (27) and its derivative, we find that $r_{\max}$ follows:

$$f_1 Z_r^{\max} + f_2 (Z_r^{\max})^3 = (4\pi)^{-3/2} \Pi_\Theta^{-1}. \tag{28}$$

When the right-hand term is small, r is bounded by $(4\pi)^{-3/2}/f_1\Pi_\Theta$ and we can compute $Z_a^{\min}$ by approximating $f_1 r^2 + f_2 r^4 \approx f_1 r^2$ in (27) to obtain

$$Z_a^{\min} \approx \frac{2^{7/2}\pi}{3} f_1^{1/2} \Pi_\Theta. \tag{29}$$

If $k = 1$, the maximum expansion of the toy-universe will be on the border of the forbidden zone (there, $a_t = 0$). Therefore, $Z_a^{\min}$ is the characteristic length scale related to the maximal expansion of the toy-universe.

4. The hyperbolic and the elliptic regimes

In this section, we describe the typical trajectories using our eigenvalue-criteria regions. The flow field shown in Fig. 2B and numerical integration of several trajectories (data not shown) indicate that if $\Pi_\Theta \neq 0$ and $\Pi_\Theta/a^3 \gg \rho_c(f_1, f_2)$, numerical trajectories starting in zones i, ii or iii are immediately ejected to the hyperbolic (real eigenvalues) region iv. On the other hand, it is shown in Fig. 3 that if $\Pi_\Theta = 0$ the forbidden region will contain all i, ii and iii zones when $a \to 0$. The early evolution of a typical trajectory is therefore expected to occur within region iv. This hyperbolic region will be studied in the first part of this section.

As $a(t)$ grows, the trajectory will eventually enter zone iii and continue to approach zone ii. Once inside the elliptic zone ii, the trajectories remain within, oscillating about the $r = r_t = 0$ axis (see Fig. 2D). This later evolution of the toy-cosmology is studied in the second part of this section.

4.1. Inflationary behavior in the hyperbolic zone

Several observational facts in physical cosmology suggest that, during an early period of evolution, the universe grew in a nearly exponential way ($a(t) \sim e^{kt}$) [9,14,15]. This inflationary period is usually introduced in standard model cosmologies through the *slow roll-over* (SRO) conditions which consist in neglecting r_{tt} and imposing a so-called vacuum-dominated energy [15,16]. To impose a vacuum-dominated energy in our system, we neglect all terms in the Hamiltonian (16) other than the expansion term $2\pi\Pi_a^2/3a$ and the potential energy term $a^3 f(r^2)$.

On the other hand, in terms of the eigenvalue-criteria regions, we expect exponential behavior to happen mainly in zone iv, where all eigenvalues are real. We thus obtain a new criterion for inflation which will be compared in the present section to the standard SRO conditions.

Let us first express the SRO conditions in terms of the reduced phase-space coordinates a, a_t and r_t. Defining $\delta_1 \equiv r_{tt}$, we can use the adimensionalized form of relations (10), (12) and (13) to map δ_1 to the reduced phase-space obtaining

$$r_t^4 + \left(2f - \frac{3k}{4\pi a^2} + \frac{\Pi_\Theta^2}{a^6 r^2}\right) r_t^2 - \frac{1}{12\pi(1+\delta_1)^2}\left(2r f' - \frac{\Pi_\Theta^2}{a^6 r^3}\right)^2 = 0. \tag{30}$$

In the limit, where $r_{tt} = \delta_1 = 0$, and the terms Π_Θ/a^3 and $3k/4\pi a^2$ are neglected (considering that they have vanished due to the exponential behavior of $a(t)$), (30) is reduced to

$$r_t^2 = -f(r^2) + \sqrt{f(r^2)^2 + \frac{r^2}{3\pi} f'(r^2)^2}. \tag{31}$$

The second SRO condition consists in supposing that the energy in (16) is dominated by the vacuum energy. It can be directly mapped to the reduced phase-space as

$$\delta_2 \equiv \frac{r_t^2}{2f(r^2)} \ll 1. \tag{32}$$

We are now in position to compare the SRO conditions [15] to the eigenvalue-criteria regions.

In Fig. 4, the evolution on the (r, r_t) plane of a typical trajectory (dotted line ABCD), with $f(r^2) = f_1 r^2 + f_2 r^4$, $f_1 = f_2 = \frac{1}{2}$ and $\Pi_\Theta = 0$, is shown. The SRO conditions, (31) and (32) (where the tolerance for condition (32) was fixed to $\delta_2 = 0.1$), are respectively labeled as SR1 and SR2. They are obeyed by trajectories in the vicinity of SR1 and between SR2 and the r axis. The eigenvalue-criteria zones are noted as ii–iv, following the convention in Fig. 1.

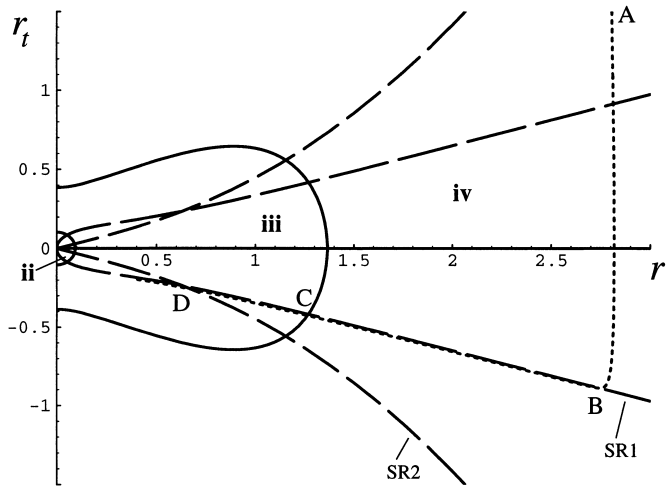

Fig. 4. Projection to the (r, r_t) plane of the reduced phase-space with $\Pi_\Theta = 0$, $f(r^2) = f_1 r^2 + f_2 r^4$ and $f_1 = f_2 = \frac{1}{2}$. The solid lines are the frontiers between ii–iv eigenvalue-criteria regions (as labeled in Fig. 1). The standard SRO conditions for inflation are satisfied when a trajectory is found near the SR1 curve and between SR2 (plotted here for a small $\delta_2 = 0.1$ tolerance criterion — see Eq. (32)) and the r axis. The dotted line shows the numerical time integration of Eqs. (10) and (14) producing a typical trajectory that first follows an adaptation transient (AB), then an inflationary regime (BC), and finally enters transition zone iii. Time integration was stopped shortly after D for numerical reasons.

The ABC segment of the trajectory occurs within the hyperbolic zone iv. According to the eigenvalue-criteria, it is expected to follow an exponential behavior. Through numerical integration we observe that all typical trajectories in this zone will first adjust to the inflationary regime after transient (segment AB on the displayed trajectory). Indeed, due to the stretching and contracting eigenvector directions corresponding to the real eigenvalue pairs that characterize zone iv, typical trajectories will closely pack in the vicinity of the SR1 curve (segment BC on the displayed trajectory). The hyperbolic zone iv therefore contains the inflationary trajectories, and defines a region where the typical evolution will rapidly lead the system to an inflationary behavior.

As the evolution continues, the trajectory enters zone iii where all eigenvalues have nonzero real and imaginary parts. In this zone, the eigenvalue-criteria does not give a clear indication on the expected type of evolution. Nevertheless, it is reasonable to consider this zone as a transition region where trajectories exit from inflation, since the system continues to evolve towards the purely imaginary eigenvalue zone ii. On the other hand, the SRO conditions does not determine a precise criterion to exit inflation since we can arbitrarily fix the tolerance δ_2 on condition (32). In Fig. 4, $\delta_2 = 0.1$ fixes the exit from inflation at point D, while $\delta_2 = 0.05$ would shift the intersection between SR1 and SR2 to the right, and make the exit from inflation to be at point C. However, it is clear that as the trajectory approaches zone ii, it no longer follows an inflationary behavior since we then have $\delta_2 \sim 1$. Zone iii therefore determines, without the δ_2 tolerance ambiguity appearing in the SRO conditions, a transition zone where the trajectory exits from inflation.

4.2. Adiabatic invariance in the elliptic zone

In this section, we study the typical evolution of the toy-cosmology within the elliptic zone ii. We will consider trajectories in the phase space that present fast oscillations about the minimum of the potential energy $V_{\text{eff}}(r^2)$ defined on relation (26), while a grows adiabatically. If $\Pi_\Theta \neq 0$, the minimum fixes the amplitude of the complex field to $r = r_0$. We will consider in this case (that will be studied in the first part of this section) nearly circular

trajectories on the complex plane, in which the phase $\Theta(t)$ turns while $r \sim r_0$. If $\Pi_\Theta \approx 0$, the minimum occurs close to $r = 0$. This case (that will be studied in the second part of this section) corresponds to highly elliptical trajectories of the field $\Phi(t)$ on the complex plane.

4.2.1. Nearly circular trajectories

When $\Pi_\Theta \neq 0$, the potential energy $V_{\text{eff}}(r^2)$ in (26) presents a minimum at $r = r_0$. In the minimal nonlinear case where $f(r^2) = f_1 r^2 + f_2 r^4$, r_0 satisfies

$$2 f_2 r_0^6 + f_1 r_0^4 - \frac{\Pi_\Theta^2}{2\,a^6} = 0. \tag{33}$$

Rather than writing all exact solutions for r_0 of the bicubic equation (33), we find the relevant solution when $\Pi_\Theta / a^3 \ll 1$. This condition is satisfied for the late evolution of the toy-cosmology. The series expansion on Π_Θ / a^3 gives

$$r_0^2 = \frac{\Pi_\Theta}{\sqrt{2 f_1} a^3} - \frac{f_2}{2 f_1^2} \left(\frac{\Pi_\Theta}{a^3} \right)^2 + \mathrm{O}\left(\frac{\Pi_\Theta}{a^3} \right)^3. \tag{34}$$

We consider trajectories that present small oscillations about r_0. The frequency ω_c of this oscillations is computed using (16), (26) and (33). One finds

$$\omega_\mathrm{c}^2 = 8 f_1 + 24 f_2 r_0^2. \tag{35}$$

Using the adiabatic invariants theory [17] one can relate the amplitude of small oscillations A_c to the characteristic size of the toy-universe a. For a slowly varying a, the adiabatic invariant is

$$I_\mathrm{c} = \tfrac{1}{2} a^3 \omega_\mathrm{c} A_\mathrm{c}^2. \tag{36}$$

Therefore, since I_c is approximately constant, the amplitude of harmonic oscillations vanishes as $a^{-3/2}$.

By comparing to the leading term in (34), we see that as a grows, A_c and r_0 vanish with the same law. The relative size of the perturbations with respect to the radius of the quasi-circular orbits traced by $\Phi(t)$ on the complex plane remains constant. This is probably not true when we consider higher than harmonic terms in the potential, which cannot be neglected for large oscillation amplitudes. If higher order effects make A_c vanish faster than $a^{-3/2}$, elliptic $\Phi(t)$ orbits would be circularized as a grows. A detailed study of these effects will be left for a future work.

In Fig. 5A, the solid line is a plot of $r(t) - r_0(t)$ (i.e. the oscillations of r about the minimum of the potential V_{eff}) for a typical numerical trajectory with $\Pi_\Theta = 10$, $f(r^2) = f_1 r^2 + f_2 r^4$, $\Pi_\Theta / a^3 \ll \rho_\mathrm{c}(f_1, f_2)$ and $f_1 = f_2 = \frac{1}{2}$. The dotted vertical lines are traced every half-period associated to the frequency $\omega_\mathrm{c} = 2$ obtained from (35). The dashed curve shows a fit of the amplitude $A_\mathrm{c}(a)$, using the law $A_\mathrm{c}(a) = K_\mathrm{c} a^{-3/2}$, as suggested by relation (36). Both analytical results are shown to give good approximations of the period and amplitude of the numerical trajectory.

We now interpret the nearly circular orbits in terms of the hydrodynamical description presented in Section 2, by computing (A.19)–(A.22). For an ideal circular orbit (with $A_\mathrm{c}(a) = 0$ and $r(t) = r_0$) we obtain

$$P_{\text{bar}} = f_2 r_0^4, \tag{37}$$

$$\varepsilon_{\text{bar}} = \frac{\Pi_\theta^2}{a^6 r_0^2} - f_2 r_0^4 = 2 f_1 r_0^2 + 3 f_2 r_0^4, \tag{38}$$

$$P_{\text{dis}} = \varepsilon_{\text{dis}} = \mathcal{T}_{\text{dis}} = 0.$$

Since all the dispersive terms vanish, the circular orbits regime is equivalent to a standard cosmology filled with a perfect barotropic fluid (see Section 2).

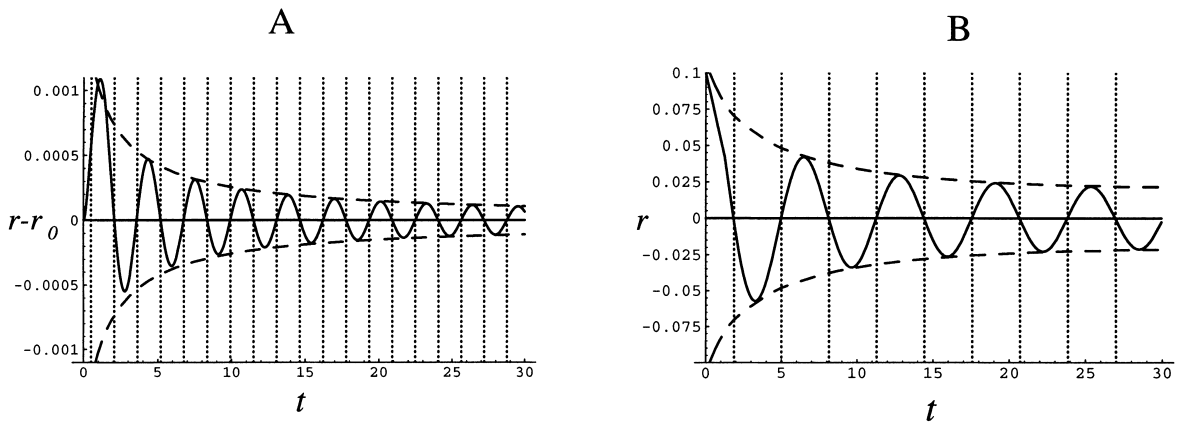

Fig. 5. Solid lines: oscillations of the amplitude $r(t)$ about the minimum of the potential $V_{\text{eff}}(r^2)$ obtained by the numerical time integrations of Eqs. (10) and (14), with $f(r^2) = f_1 r^2 + f_2 r^4$, $f_1 = f_2 = \frac{1}{2}$. In (A), we show the nearly circular case with $\Pi_\Theta = 10$, where the minimum of $V_{\text{eff}}(r^2)$ is at $r = r_0$, as computed from (33). In (B), we show the highly elliptic regime limit with $\Pi_\Theta = 0$, where the minimum of $V_{\text{eff}}(r^2)$ is at $r = 0$. Vertical dotted lines: analytical approximation of the half-period of the frequency given by Eqs. (35) and (42). Dashed lines: analytical fits of the amplitude of small oscillations using the $a(t)^{-3/2}$ law obtained by using the adiabatic invariants (see text).

An exact implicit expression for the equation of state can be found by solving Eqs. (37) and (38). We find

$$P_{\text{bar}} + \frac{2}{3} f_1 \sqrt{\frac{P_{\text{bar}}}{f_2}} = \frac{\varepsilon_{\text{bar}}}{3}. \tag{39}$$

This relation describes the fluid's thermodynamical behavior on the circular orbits regime.

An approximate expression of the fluid's equation of state after a large expansion ($\Pi_\theta / a^3 \ll 1$) is found by expanding (37) and (38) in powers of Π_θ / a^3. One obtains

$$P_{\text{bar}} = \frac{f_2}{2 f_1} \left(\frac{\Pi_\theta}{a^3} \right)^2 + \text{O} \left(\frac{\Pi_\Theta}{a^3} \right)^3, \tag{40}$$

$$\varepsilon_{\text{bar}} = \sqrt{2 f_1} \left(\frac{\Pi_\theta}{a^3} \right) + \frac{f_2}{2 f_1} \left(\frac{\Pi_\theta}{a^3} \right)^2 + \text{O} \left(\frac{\Pi_\Theta}{a^3} \right)^3. \tag{41}$$

To leading order, these relations reduce to the equation of state for a dust gas $P_{\text{bar}} = 0$. This is in agreement with what one expects for a toy-universe after a large expansion, since then the density is low, so the interactions can be neglected and the energy is dominated by the rest mass.

4.2.2. Highly elliptical trajectories

We will focus here on the limit of highly elliptic ($\Pi_\Theta \approx 0$) orbits. In this case, the minimum of the potential $V_{\text{eff}}(r^2)$ in (26), with $f(r^2) = f_1 r^2 + f_2 r^4$, is trivially found to be at $r = 0$. Repeating the same computations as in Section 4.2.1, the oscillation frequency of highly elliptical orbits is

$$\omega_{\text{e}}^2 = 2 f_1, \tag{42}$$

while the adiabatic invariant is

$$I_{\text{e}} = \tfrac{1}{2} \sqrt{2 f_1} a^3 A_{\text{e}}^2, \tag{43}$$

so the amplitude of harmonic oscillations A_e also vanishes as $a^{-3/2}$. In Fig. 5B the solid line shows the oscillations of $r(t)$ for a typical numerical trajectory with $\Pi_\Theta = 0$, $a \gg 1$, $f(r^2) = f_1 r^2 + f_2 r^4$ and $f_1 = f_2 = \frac{1}{2}$. The dotted vertical lines are traced every half-period associated to the frequency $\omega_e = 1$ obtained from (42). The dashed curve shows a fit of the amplitude A_e, using the law $A_e = K_e a^{-3/2}$, as suggested by relation (43). Both analytical results are shown to give good approximations of the period and amplitude of the numerical trajectory.

Finally, we search for an hydrodynamical interpretation of the highly elliptic orbits by taking the time average of (A.19)–(A.22) over the oscillations of the rapid dynamical variable $r(t)$. By directly replacing $r(t) = A_e \cos(\omega_e t)$ we compute $\omega_e \int_0^{2\pi/\omega_e} dt/2\pi$ (which we will denote by $\langle\cdot\rangle$). We obtain

$$\langle P_{bar}\rangle = \tfrac{3}{8} f_2 A_e^4, \qquad \langle \varepsilon_{bar}\rangle = -\tfrac{3}{8} 3 f_2 A_e^4, \qquad \langle P_{dis}\rangle = \langle \varepsilon_{dis}\rangle = 0, \qquad \langle \mathcal{T}_{dis}\rangle = \tfrac{1}{2} A_e^2 \omega^2.$$

Since $\langle \mathcal{T}_{dis}\rangle$ dominates when A_0 is small, the quantum pressure effects are important and we cannot identify this system with a relativistic fluid as we had done in the nearly circular case. This can be related to the fact that, at an early evolution stage, the quantum terms become important and therefore the complex matter field is not expected to follow a barotropic fluid behavior.

5. Discussion and conclusions

The purpose of this section is to discuss the general significance of the results obtained through the detailed study of the toy-cosmology described by the Lagrangian (15). In Section 3, we were able to classify different regions of the phase space according to the evolution of the separation between nearby points. The classification was made possible by the determination of the eigenvalues of the tangent map as pioneered by Weiss [10] in a simpler context. In Section 4, we showed that inflationary behavior occurs in hyperbolic regions, while classical behavior could be obtained in elliptic regions through an adiabatic approximation. This qualitative picture is expected to be robust in the sense that the same behaviors will occur even when more complicated field Lagrangians are used. It therefore seems fit to locate our results in the current panorama of physical cosmology.

Physical cosmology is primarily interested by the large scale structure of the real universe we live in. For various reasons which need not be reviewed here, many cosmologists have reached the conclusion that our universe might very well have experienced in the past a phase where all sizes exponentially increased with time (in contradiction with the predictions of the standard FRW models, where the scale dependence on time obeys a power law). Such a period is referred to as inflation [9,16]. It is usually supposed that this inflation was driven by some unknown field, conveniently called inflaton and that, after some time, inflation ceased when the inflaton decayed into some lighter particles, allowing our universe to enter a FRW phase. In practical calculations, the inflaton is usually taken to be a real neutral first quantized Klein–Gordon field but the theoretical possibility of generating inflation with other kinds of matter field has already been mentioned.

From that point of view, it would be tempting to interpret some of the results presented in this paper as a new implementation of the inflation idea. We do not consider our work that way for the following reasons. For physical cosmology, studying in detail some solutions of the Einstein equations, albeit cosmological ones, is but one issue. Physical cosmology has also to cope, inter alia, with high energy physics and quantum gravity on the theoretical side, and with condensed matter physics and statistical data analysis on the experimental one. Our aim was certainly not to present some results pertaining to theoretical physical cosmology. We have restricted our attention to a well-defined problem in theoretical physics, i.e. the study of the generic behavior of solutions to a system of nonlinear equations which represents, in purely physical terms, the minimal coupling between Einsteinian gravity and a charged Klein–Gordon field. That this generic behavior seems to include a phase which deserves the name inflation might be striking, as might be the fact that the system under consideration seems to exit spontaneously from

that inflationary period. Even if these points can be interpreted as possible hints to some perhaps simpler models of the early evolution of our universe, the system investigated in this paper is certainly not to be considered as a real cosmological model but, at best, a toy-model for future realistic cosmologies. It is our feeling that the prevalence of an inflationary phase followed by a FRW type evolution are best understood with the modern nonlinear concepts of robustness and genericity.

Appendix A

We will now briefly present a hydrodynamical description of the matter field Φ. It has been shown in [8,18] that we can map Φ to a set of standard hydrodynamical variables: n (the particle number density or barionic number density), u^μ (the fluid's 4-velocity), w (the enthalpy density) and P (the pressure). These variables obey dynamical equations which are essentially equivalent to the ideal barotropic relativistic fluid expressions (except for supplementary dispersive terms which are commonly called quantum pressure terms). A formal correspondence between (5) and a relativistic potential flow can be achieved by using the Madelung transform [4,5]:

$$\Phi = r \exp\left(\mathrm{i}\frac{\Theta}{2\alpha}\right), \tag{A.1}$$

where we define

$$u^\mu = \frac{-\nabla^\mu\Theta}{(\nabla_\beta\Theta\nabla^\beta\Theta)^{1/2}}, \qquad n = \frac{r^2}{m_\mathrm{b}c}(\nabla_\beta\Theta\nabla^\beta\Theta)^{1/2}, \qquad w = r^2(\nabla_\beta\Theta\nabla^\beta\Theta). \tag{A.2}$$

From these definitions we obtain the standard special relativistic condition for potential flows and the conservation of the current associated to the $U(1)$ phase invariance of $\mathcal{A}$ becomes the usual continuity equation in relativistic hydrodynamics

$$\nabla_\mu(nu^\mu) = 0. \tag{A.3}$$

Using (A.2) and the real part of the product by Φ^* of the NLKG equation, [1] we find the following expressions for n and w in terms of r:

$$n = \frac{r}{m_\mathrm{b}c}(4\alpha r^2 f'(r^2) + 4\alpha^2 r\nabla_\beta\nabla^\beta r)^{1/2}, \qquad w = 4\alpha r^2 f'(r^2) + 4\alpha^2 r\nabla_\beta\nabla^\beta r. \tag{A.4}$$

The terms containing $\nabla_\beta\nabla^\beta r$ reflect the dispersive nature of the fluid and correspond to the so-called *quantum pressure* terms. If they are neglected, it is possible to deduce from (A.4) the correct expression for the pressure of the remaining barotropic fluid P_bar, making use of the standard thermodynamical relation for systems with vanishing entropy $\mathrm{d}P_\mathrm{bar} = n\,\mathrm{d}h$, where h is the enthalpy per particle ($h = w/n$). We thus obtain

$$P_\mathrm{bar} = 2\alpha(r^2 f'(r^2) - f(r^2)). \tag{A.5}$$

It is also convenient to introduce, according to (A.4):

$$w_\mathrm{bar} = 4\alpha r^2 f'(r^2), \tag{A.6}$$

and the internal energy density ε_bar through the usual thermodynamic relation:

$$\varepsilon_\mathrm{bar} = w_\mathrm{bar} - P_\mathrm{bar}. \tag{A.7}$$

[1] The imaginary part gives back Eq. (A.3).

We are now in position to cast $T^{\mu\nu}$ in a close-to-standard-relativistic-hydrodynamics form

$$T^{\mu\nu} = (w + w_{\rm dis})u^\mu u^\nu - (P_{\rm bar} + P_{\rm dis})g^{\mu\nu} + \mathcal{T}^{\mu\nu}_{\rm dis}. \tag{A.8}$$

The dispersive parts of the enthalpy density $w_{\rm dis}$ and pressure $P_{\rm dis}$ are then given by

$$w_{\rm dis} = 4\alpha^2 r\nabla_\beta\nabla^\beta r, \tag{A.9}$$

$$P_{\rm dis} = \alpha^2\nabla_\beta\nabla^\beta r^2, \tag{A.10}$$

and the only dispersive term in the $T^{\mu\nu}$ that does not have a barotropic analog is

$$\mathcal{T}^{\mu\nu}_{\rm dis} = 4\alpha^2\nabla^\mu r\nabla^\nu r. \tag{A.11}$$

Finally, we consistently define the dispersive internal energy density as

$$\varepsilon_{\rm dis} = w_{\rm dis} - P_{\rm dis}. \tag{A.12}$$

The hydrodynamical formulation provides us with a physical interpretation for f_1 and f_2. From (A.5) and (A.7) we can see that, to leading order, f_1 and f_2 fix respectively the internal barotropic internal energy density $\varepsilon_{\rm bar}$ and the barotropic pressure $P_{\rm bar}$. In the minimal nonlinear case where $f(r^2) = c^2 f_1 r^2/2\alpha + 2G\alpha f_2 r^4/c^2$, $P_{\rm bar}$ is simply given by

$$P_{\rm bar} = \frac{4\alpha^2 G}{c^2} f_2 r^4, \tag{A.13}$$

and therefore f_2 determines this equation of state for the barotropic fluid part uniquely. We also obtain from the hydrodynamical interpretation two characteristic scales that could presumably be relevant to the evolution of the toy-model studied in Sections 3 and 4: the speed of sound $c_{\rm s}$ and the length scale ξ at which dispersion becomes noticeable (known as the *coherence length*). We can roughly estimate these two quantities using their nonrelativistic expressions $c_{\rm s} = \sqrt{2\alpha r^2 f''(r^2)}$ and $\xi = \sqrt{\alpha/(r^2 f''(r^2))}$ given in [6,7] and obtain, in the minimal nonlinear case

$$c_{\rm s} = \frac{(6 f_2 G)^{1/2}\alpha}{c} r, \tag{A.14}$$

$$\xi = \frac{c}{2(f_2 G)^{1/2}} r^{-1}. \tag{A.15}$$

Before ending this section, let us point out that the Madelung transform (A.1) can only be used in situations where the complex matter field Φ contains no vortices [8] since the phase Θ is not defined when $r = 0$. However, it has been shown in [18] that a phase-amplitude (Θ, r) representation of the field is not required to define w, P and ε, thus permitting the hydrodynamical interpretation to be established even in the presence of vortices.

Using homogeneity, we can readily show from (A.2) that for the homogeneous and isotropic cosmology considered in this paper, the 4-velocity u^μ is constant and given by $u^0 = 1$ and $u^1 = u^2 = u^3 = 0$. In the same way, the barionic number n and the enthalpy density w are given by

$$n = \frac{r^2}{m_{\rm b}c^2}\Theta_t, \qquad w = \frac{r^2}{c^2}\Theta_t^2, \tag{A.16}$$

where the subscript t indicates a time derivative. The continuity equation (A.3) furnishes the conservation relation

$$\partial_t(a^3 r^2 \Theta_t) = 0, \tag{A.17}$$

which had already been obtained from the NLKG equation (see Eq. (11)). The conserved quantity Π_Θ, defined in expression (12), can therefore be expressed as

$$\Pi_\Theta = m_\mathrm{b}\, a^3 n. \tag{A.18}$$

Eq. (A.17) amounts to the conservation of the number of particles or barions contained in the characteristic volume a^3. In particular, when $k = 1$ (i.e. for a closed and therefore finite universe), the total volume of the universe is $2\pi^2 a^3$, so the total barion number N_b is given by $N_\mathrm{b} = 2\pi^2 a^3 n = 2\pi^2 \Pi_\Theta / m_\mathrm{b}$.

We can also derive explicit expressions to be used below for the pressure and the internal energy density. Using (A.5), (A.6) and (A.7), we obtain

$$P_\mathrm{bar} = 2\,\alpha\, \left(r^2\, f'(r^2) - f(r^2) \right), \tag{A.19}$$

$$\varepsilon_\mathrm{bar} = 4\alpha r^2 f'(r^2) - P_\mathrm{bar} = 2\,\alpha (r^2\, f'(r^2) + f(r^2)), \tag{A.20}$$

while (A.9), (A.10) and (A.12) produce

$$P_\mathrm{dis} = \frac{2\,\alpha^2}{c^2} \left(3\,\frac{a_t}{a}\, r\, r_t + r_t^2 + r\, r_{tt} \right), \tag{A.21}$$

$$\varepsilon_\mathrm{dis} = \frac{4\alpha^2 r}{c^2} \left(r_{tt} + 3\frac{a_t}{a} r_t \right) - P_\mathrm{dis} = \frac{2\,\alpha^2}{c^2} \left(3\,\frac{a_t}{a}\, r\, r_t - r_t^2 + r\, r_{tt} \right). \tag{A.22}$$

For the FRW case, we therefore obtain, in the reference frame where the metric takes the form (9), a simple diagonal form for $T^{\mu\nu}$: $T^{\mu\nu} = \mathrm{diag}(T^{tt}, T^{ll}, T^{ll}, T^{ll})$, where $T^{ll} = P_\mathrm{bar} + P_\mathrm{dis}$ and $T^{tt} = \varepsilon_\mathrm{bar} + \varepsilon_\mathrm{dis} + \mathcal{T}_\mathrm{dis}$, with

$$\mathcal{T}_\mathrm{dis} = \frac{4\,\alpha^2\, r_t^2}{c^2}. \tag{A.23}$$

References

[1] E.P. Gross, Nuovo Cimento 20 (1961) 454.
[2] L.P. Pitaevskii, Soviet Phys. JETP 13 (1961) 451.
[3] L. Landau, E. Lifschitz, Physique Statistique, Vol. 9, Editions Mir, Moscow, 1990.
[4] E.A. Spiegel, Fluid dynamical form of the linear and nonlinear Schrödinger equations, Physica D 1 (1980) 236.
[5] R.J. Donnelly, Quantized Vortices in Helium II, Cambridge University Press, Cambridge, 1991.
[6] C. Nore, M. Abid, M. Brachet, Decaying Kolmogorov turbulence in a model of superflow, Phys. Fluids 9 (9) (1997) 2644.
[7] M. Abid, M.E. Brachet, F. Debbasch, C. Nore, Galilean and relativistic nonlinear wave equations: an hydrodynamical tool? In: E. Tirepegui, W. Zeller (Eds.), Instabilities and Nonequilibrium Structures, Vol. V, Kluwer Academic Publishers, Netherlands, 1997.
[8] F. Debbasch, M.E. Brachet, Relativistic hydrodynamics of semiclassical quantum fluids, Physica D 82 (1995) 255.
[9] R. Wald, General Relativity, University of Chicago Press, Chicago, 1984.
[10] J. Weiss, The dynamics of enstrophy transfer in two-dimensional hydrodynamics, Physica D 48 (1991) 273–294.
[11] V. Arnold, Mathematical Methods of Classical Mechanics, Vol. 60, Springer, New York, 1978.
[12] I.M. Khalatnikov, A. Mezhlumian, The classical and quantum cosmology with a complex scalar field, Phys. Lett. A 169 (1992) 308–312.
[13] I.M. Khalatnikov, A.Yu. Kamenshchik, Singularity, initial conditions, quantum tunneling and scalar field in modern cosmology, Phys. Rep. 288 (1997) 513–543.
[14] M.S. Turner, E.W. Kolb, The Early Universe, Addison-Wesley, Redwood City, 1990.
[15] R. Domingues-Tenreiro, M. Quirós, An Introduction to Cosmology and Particle Physics, World Scientific, Singapore, 1988.
[16] A.D. Linde, Phys. Lett. B 129 (1983) 177.
[17] L. Landau, E. Lifschitz, Mécanique, Vol. 1, Editions Mir, Moscow, 1982.
[18] C. Huepe, F. Debbasch, M.E. Brachet, Hydrodynamical interpretation of relativistic charged scalar field dynamics, in: M. Signore, F. Melchiorri (Organizers), Proceedings of the Conference: Topological Defects in Cosmology, Rome, October 1996, 1997.